# Lipopolysaccharide Neutralizing Peptide−Porphyrin Conjugates for Effective Photoinactivation and Intracellular Imaging of Gram-Negative Bacteria Strains

Fang Liu,[†] Annie Soh Yan Ni,[†] Yingjie Lim,[†] Harini Mohanram,[‡] S. Bhattacharjya,*[,‡] and Bengang Xing*[,†]

[†]Division of Chemistry & Biological Chemistry, School of Physical & Mathematical Sciences, and [‡]Division of Structural and Computational Biology, School of Biological Physical Sciences, Nanyang Technological University, Singapore 637371

Ⓢ *Supporting Information*

ABSTRACT: A simple and specific strategy based on the bioconjugation of a photosensitizer protophophyrin IX (PpIX) with a lipopolysaccharide (LPS) binding antimicrobial peptide YI13WF (YVLWKRKRKFCFI-Amide) has been developed for the effective fluorescent imaging and photodynamic inactivation of Gram-negative bacterial strains. The intracellular fluorescent imaging and photodynamic antimicrobial chemotherapy (PACT) studies supported our hypothesis that the PpIX-YI13WF conjugates could serve as efficient probes to image the bacterial strains and meanwhile indicated the potent activities against Gram-negative bacterial pathogens especially for those with antibiotics resistance when exposed to the white light irradiation. Compared to the monomeric PpIX-YI13WF

conjugate, the dimeric conjugate indicated the stronger fluorescent imaging signals and higher photoinactivation toward the Gram-negative bacterial pathogens throughout the whole concentration range. In addition, the photodynamic bacterial inactivation also demonstrated more potent activity than the minimum inhibitory concentration (MIC) values of dimeric PpIX-YI13WF conjugate itself observed for *E. coli* DH5a (∼4 times), *S. enterica* (∼8 times), and other Gram-negative strains including antibiotic-resistant *E. coli* BL21 (∼8 times) and *K. pneumoniae* (∼16 times). Moreover, both fluorescent imaging and photoinactivation measurements also demonstrated that the dimeric PpIX-YI13WF conjugate could selectively recognize bacterial strains over mammalian cells and generate less photo damage to mammalian cells. We believed that the enhanced fluorescence and bacterial inactivation were probably attributed to the higher binding affinity between dimeric photosensitizer peptide conjugate and LPS components on the surface of bacterial strains, which were the results of efficient multivalent interactions.
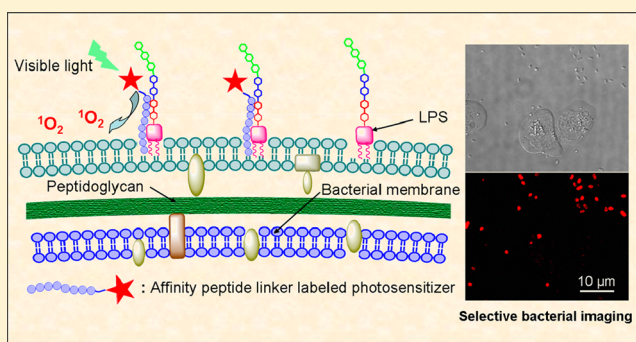
INTRODUCTION

Since penicillin was first introduced into medical practice in the 1940's, a large number of various antibiotics have been developed to successfully inhibit bacterial infection diseases in clinics. However, increasing bacteria resistance to most of antibiotics has been extensively reported in medical treatment and has currently emerged as a serious threat to public health.[1−6] As such, there is an emergent need to design new types of antimicrobial agents and alternative treatment strategies that can effectively kill the bacterial strains with potent drug-resistant properties. One promising approach for microbiological inactivation is based on photodynamic antimicrobial chemotherapy (PACT), by which porphyrins or related compounds such as photofrin and foscan have been employed as photosensitizers (PS) to activate reactive oxygen species (ROS, e.g., singlet oxygen ($^1O_2$)) when exposed to room light with a suitable wavelength. The activated singlet oxygen species can be used as highly reactive oxidants and are capable of destroying the cell walls and membranes in close proximity, thus resulting in cell death.[7−13] In the process of

PACT, the effective affinity of the photosensitizers on the surface of target bacterial cells would be crucial to enable the potent photoinactivation against bacterial strains. One possible antimicrobial strategy to minimize the side effects and enhance the potency of bacterial PACT inactivation is the utility of affinity ligands, which can selectively deliver the PSs to the targeted bacterial infection sites and lead to bacterial killing with minimum nonspecific drug accumulation.[14−16] So far, several affinity ligand conjugated photosensitizer complexes have been used to successfully inactivate a variety of antibiotic-resistant pathogens, especially for those methicillin-resistant *Staphylococcus aureus* (MRSA) and vancomycin-resistant *enterococci* (VRE).[17−25] However, most of the existing photosensitizer systems based on affinity ligands only exhibit efficient antimicrobial activity against Gram-positive strains rather than Gram-negative ones mostly due to the presence of a highly

organized outer bacterial membrane structure with a highly negatively charged lipid portion, which blocks the cellular attachment between PS and bacteria and thus intercepts $^1O_2$.[26] Although several affinity ligands based on nanoparticles[18] and water-soluble conjugated polymers[19,25] and polypeptides[20] have been recently developed to achieve close association of PSs to the Gram-negative bacterial strains and have indicated effective photoinactivation toward these strains, the development of simple and specific affinity ligand molecules that can selectively direct photosensitizers to the surface of Gram-negative bacteria pathogens is of great importance and remains the challenge in the antimicrobial studies, since the current approaches may indicate potential disadvantages including tedious sample treatment, nonspecific aggregation, possible immune response, or less cellular penetration.

Generally, Gram-negative bacteria are characterized by two distinct lipid membrane structures, one is an inner membrane consisted of glycerophospholipids and the other is an asymmetric bilayer outer membrane predominantly composed of a highly conserved and chemically unique lipopolysaccharide (LPS) moiety. The amphiphilic LPS contains one lipid A, a lipid fragment with six or seven fatty-acid-acylated chains, and a few hydrophilic polysaccharides components with negatively charged phosphate and carboxyl groups, which have been considered an efficient barrier to prevent bacterial pathogen strains from the permeability of antimicrobial molecules including hydrophobic antibiotics, surfactants, host-defense proteins, and peptides.[27−29] Apart from the function as the major constituent of the outer membrane of Gram-negative bacteria, LPS has also been considered as one of the most potent bacterial signal molecules that can strongly stimulate the host defenses to release proinflammatory mediators and often result in endotoxic shock or sepsis in intensive care units.[30−32] One promising strategy to inhibit septic shock will be the rational development of functional antimicrobial peptides, the ubiquitous arsenals of all living organisms, which would bind with LPS with a high affinity and significantly block the interactions between LPS and its recognition protein receptors. So far, extensive studies have been recently carried out to investigate the interactions of antimicrobial peptides toward LPS for their important roles in antibacterial activation, outer membrane perturbation, and LPS neutralization.[33−37]

In this study, we report a simple and effective dimeric peptide porphyrin binding system, by which a cationic antimicrobial peptide with the sequence of YVLWKRKRKFCFI-Amide (YI13WF) was chosen as a bacterial affinity ligand to link with a most commonly used porphyrin photosensitizer (PpIX). This new dimeric antimicrobial PpIX−peptide conjugate may indicate a unique advantage to selectively adhere to the surface of Gram-negative bacterial strains based on the enhanced multivalent/polyvalent interactions between disubstituted peptides and LPS moieties on bacterial strains, and thus serve as a promising fluorescent probe and potent photosensitizer for specific imaging and photodynamic inactivation of drug-resistant Gram-negative bacterial strains.

■ EXPERIMENTAL PROCEDURES

General. All the chemical reagents were purchased from Sigma Aldrich or Fluka. Commercially available reagents were used without further purification. The antimicrobial peptides were synthesized commercially by GL Biochem (Shanghai, China) and further purified by reverse-phase HPLC. All bacterial strains were from American Type Culture Collection (ATCC), USA. ^1H NMR spectra were recorded using either a Bruker 300 or 400 MHz spectrometer. Mass spectra (MS) were measured with a Thermo LCQ Deca XP Max for ESI. Analytical reverse-phase HPLC analysis was performed on a Shimadzu HPLC system using an Alltima C-18 (250 × 10 mm) column at a flow rate of 2.5 mL/min for preparation and a C-18 (250 × 4.6 mm) for analysis. Fluorescence emission spectra were performed on a Varian Cary eclipse Fluorescence spectrometer. UV absorption spectra were recorded in a 5 mm path quartz cell on a Beckman coulter DU 800 spectrometer. Photoirradiation experiments were performed at a fluence rate of 50 mW/cm^2 with a cool-light fiber optic illuminator provided by a 150 W OSRAM Quartz Halogen bulb (400−900 nm).

Synthesis. *N-Boc-Ethylenediamine 1.* Di-*tert*-butyldicarbonate (Boc$_2$O) (10.0 g, 46 mmol) was added into a mixture of ethylenediamine (10.0 mL, 150 mmol) and triethylamine (2 mL) in 20 mL of ethanol at 0 °C. The solution was stirred for 2 h at room temperature. The solvent was then removed using a rotator evaporator and the contents were redissolved in 20 mL of dichloromethane (DCM). The solution was subsequently extracted with 1.0 M acetic acid, and the pH of the aqueous layer was adjusted to pH 9−10 using 2.0 M sodium hydroxide (NaOH). Extraction was carried out with DCM (3 × 10 mL). **1** was collected by removing the solvent and used in the next step of the synthesis without further purification (9.6 g, 40%). ^1H NMR (300 MHz, CDCl$_3$): δ 1.40 (9H, s), 2.76 (2H, t, J = 5.85 Hz), 3.12 (2H, t, J= 5.70 Hz), 5.07 (1H, s). C$_7$H$_{16}$N$_2$O$_2$, ESI-MS: m/z 160.12 (calcd); 160.84 [M+H]$^+$, 320.78 [2M+H]$^+$ (found).

N-(2-[(t-Boc)amino]ethyl Maleimide 2. Maleic anhydride (400 mg, 1.66 mmol) in 35 mL of ethanol was added dropwise into a solution of **1** (1.2 equiv) and triethylamine in 30 mL of ethanol at 0 °C and stirred for 4 h. The solvent was removed and the contents were redissolved in 8 mL of acetic anhydride. Sodium acetate (1.0 equiv) was added and the solution was heated to 60−70 °C for 30 min then cooled to room temperature. Water was added to the solution and subsequent extraction was carried out with ethyl acetate. The organic layer was collected and washed with saturated sodium bicarbonate solution. After drying with anhydrous sodium sulfate, the organic layer was concentrated and purified with flash chromatography (EA/hexanes, 1:3) to give a white solid **2** (1.2 g, 82%). ^1H NMR (300 MHz, CDCl$_3$): δ 1.40 (9H, s), 3.32 (2H, d, J = 5.4 Hz), 3.65 (2H, t, J = 5.6 Hz), 4.73 (1H, s), 6.70 (2H, s). C$_{11}$H$_{16}$N$_2$O$_4$, ESI-MS: m/z 240.11 (calcd); 240.83 [M+H]$^+$ (found).

N-(2-Aminoethyl)maleimide Trifluoroacetate Salt 3. Compound **2** (1.0 g, 4.17 mmol) dissolved in 10 mL of DCM was added with trifluoroacetic acid (TFA) (5 mL) at 0 °C and stirred for 1 h. DCM was removed by evaporation and contents were redissolved in 3 mL of methanol. The desired product was precipitated with 50 mL of diethyl ether and used without further purification.

Monomeric PpIX-Maleimide Derivative 4. Protoporphyrin IX (PpIX) (50 mg, 0.09 mmol) and *N*-hydroxysuccinimide (HOSu) (9.2 mg, 0.08 mmol, 0.9 equiv) was dissolved in 8 mL of dimethyl formamide (DMF) at 0 °C and stirred for 10 min before the addition of 1-ethyl-3-(3-dimethyl-aminopropyl) carbodiimide hydrochloride (EDC.HCl) (20.4 mg, 0.117 mmol, 1.3 equiv). The reaction mixture was stirred at room temperature for 4 h. Compound **3** (20 mg, 0.08 mmol, 0.9 equiv) was then added and the system was left to stir for a

further 5 h at room temperature. The compound was purified by flash chromatography with eluent methanol/DCM = 1:20 to give a red solid product as mixture of two regioisomers (26.2 mg, 43%) . ^{1}H NMR (400 MHz, DMSO-d_6): δ 2.92 (2H, t, J = 7.6 Hz), 3.16−3.20 (4H, m), 3.44 (2H, t, J = 5.8 Hz), 3.61 (6H, m), 3.71 (6H, m), 4.27 (2H, t, J = 7.6 Hz), 4.35 (2H, t, J = 7.2 Hz), 6.23 (2H, d, J = 11.2 Hz), 6.47 (2H, dd, J_1 = 18.0 Hz, J_2 = 2.0 Hz), 6.86 (2H, s), 8.06 (1H, s), 8.48 (2H, dd, J_1 = 17.6 Hz, J_2 = 11.6 Hz), 10.20−10.25 (4H, m). $C_{40}H_{40}N_6O_5$, ESI-MS: m/z 684.31 (calcd); 685.48 $[M+H]^+$, 1368.80 $[2M+H]^+$ (found).

Dimeric PpIX-Maleimide Derivative 5. PpIX (20 mg, 0.036 mmol) and HOSu (9.2 mg, 0.079 mmol) was dissolved in 4 mL of DMF at 0 °C, EDC.HCl (15 mg, 0.079 mmol) was then added to the reaction mixture and allowed to stirred at room temperature for 4 h. Following the addition of compound **3** (20 mg, 0.079 mmol), the system was left to stir for another 5 h at room temperature. The compound was purified by flash chromatography with eluent methanol/DCM 1:50 to give a red solid product (20.9 mg, 73%). ^{1}H NMR (400 MHz, DMSO-d_6): δ 2.95 (4H, t, J =7.6 Hz), 3.19 (4H, t, J = 6.0 Hz), 3.43 (4H, t, J =5.6 Hz), 3.61 (3H, s), 3.64 (3H, s), 3.76 (3H, s), 3.77 (3H, s), 4.29 (4H, t, J =7.2 Hz), 6.24 (2H, d, J = 11.6 Hz), 6.47 (2H, dd, J_1 = 18.0 Hz, J_2 = 4.0 Hz,), 6.80 (4H, s), 8.14 (2H, t, J = 6.0 Hz,), 8.54 (3H, m), 10.21 (1H, s), 10.29 (2H, s), 10.38 (1H, s). $C_{46}H_{46}N_8O_6$, ESI-MS: m/z 806.35 (calcd); 807.49 $[M+H]^+$, 1613.92 $[2M+H]^+$ (found).

Monomeric PpIX−Peptide Conjugate 6. Compound **4** (1.1 mg, 1.6 μmol) and peptide YI13WF (2.8 mg, 1.6 μmol) in 200 μL of dimethylsulfoxide (DMSO) were added with 5 μL DMSO solution containing 10% diisopropylethylamine (DIPEA). The mixture was allowed to stir at room temperature overnight and then was added to 10 mL diethyl ether to give a red precipitate. This crude solid was purified by reverse-phase high performance liquid chromatography (HPLC) with eluting system consisting of A (water with 0.1% TFA) and B (acetonitrile with 0.1% TFA) under a linear gradient, monitored by UV absorbance at 280 and 400 nm. The linear gradient stretched over 43 min from t = 2 min at 70% solution A and 30% solution B to t = 45 min at 20% solution A and 80% solution B. The reaction yielded a deep red solid monomeric PpIX−peptide conjugate **6** (2.3 mg 56%) after lyophilization. ^{1}H NMR (400 MHz, DMSO-d_6): δ 0.66−0.80 (m), 0.96 (br s), 1.12 (s), 1.21−1.71 (overlapped), 1.84−1.92 (m), 2.25−2.36 (m), 2.65−2.75 (overlapped), 2.76−2.92 (m), 2.81−3.15 (m), 3.57 (dd, J_1 = 10.6 Hz, J_2 = 7.2 Hz), 3.69−3.71 (m), 3.89−3.96 (m), 4.12−4.30 (m), 4.47−4.55 (m), 6.15−6.19 (m), 6.41 (d, J = 17.6 Hz), 6.56 (d, J = 8.4 Hz), 6.87−6.98 (m), 7.00−7.20 (m), 7.24 (d, J = 8.0 Hz), 7.52−7.63 (m), 7.68−7.75 (br s), 7.82−7.94 (br s), 7.96−8.21 (m), 8.42−8.52 (m), 9.15 (br s), 10.19 (s), 10.23 (s), 10.25 (s), 10.32 (s),10.70 (s). $C_{128}H_{175}N_{29}O_{20}S$, ESI-MS: $m/2z$, 1236.53, $m/3z$ 825.11, $m/4z$ 619.18, $m/5z$, 495.69 (found).

Dimeric PpIX−Peptide Conjugate 7. Compound **5** (2.0 mg, 2.5 μmol) and peptide YI13WF (10 mg) (10.0 mg, 5.6 μmol) in 200 μL of dimethylsulfoxide (DMSO) was added with 5 μL of DMSO solution containing 10% diisopropylethylamine (DIPEA). The reaction was treated as described above and the crude products were purified by reverse-phase HPLC with the same eluting system as purification of the monomeric conjugate **6**. The reaction yielded a deep red solid **7** (5.3 mg, 48%) after lyophilization. ^{1}H NMR (400 MHz, DMSO-d_6): δ 0.65−0.80 (m), 0.95 (br s), 1.12−1.74 (overlapped), 1.84−1.92 (m), 2.25−2.36 (m), 2.70 (br s), 2.83−3.15 (overlapped), 3.60

(d, J = 10.8 Hz), 3.71 (d, J = 3.6 Hz), 3.86−3.95 (m), 4.12−4.31 (overlapped), 4.35−4.55 (overlapped), 6.17 (dd, J_1 = 11.8 Hz, J_2 = 6.0 Hz), 6.42 (dd, J_1 = 18.5 Hz, J_2 = 5.4 Hz), 6.85−7.35 (m), 7.52 (d, J = 8.0 Hz), 7.60 (d, J = 4.8 Hz), 7.80 (br s), 8.10 (br s), 8.05−8.15 (m), 8.20 (br s), 8.40−8.55 (m), 9.16 (s), 10.17 (s), 10.24 (s), 10.34 (s), 10.75 (s). $C_{222}H_{316}N_{54}O_{36}S_2$, ESI-MS: m/z 4380.41(calcd); $m/3z$ 1460.97, $m/4z$ 1096.29, $m/5z$ 877.34, $m/6z$ 731.43, $m/7z$ 627.18, $m/8z$ 549.09 (found).

General Spectroscopic Measurements. 1.0 mM stock solution (in DMSO) of PpIX, conjugate **6** and **7**, was diluted to 5.0 μM in DMSO. The UV−vis spectra were recorded using a Beckman coulter DU800 spectrometer. Wavelength Interval: 1.0 nm. Scan Speed: 1200 nm/min. Fluorescence spectroscopic studies were also performed using a Varian Cary Eclipse Fluorescence Spectrophotometer at the excitation wavelength of 504 nm.

Bacterial and Cell Culture. Four Gram-negative bacteria strains: *E. coli* DH5a (ATCC 53868), *S. enterica* (ATCC 14028), and ampicillin-resistant bacterial strains *E. coli* BL21 (Amp^r *E. coli*) and *K. pneumoniae* (ATCC 700603) were used in this study. Luria−Bertani (LB) medium was used for all four bacterial strains tested in this study. A single colony from the stock LB agar plate was added to 3 mL of liquid medium, then was grown at 37 °C on a shaker incubator (200 rpm) overnight followed by a subculture until an OD_{600} of approximately 0.5−0.7 was reached.

Minimum Inhibitory Concentration (MIC) Test. Antimicrobial activities of the designed peptides were determined following a previously reported method with a light modification.[38] Briefly, 1.0 mL aliquots of bacterial strains cultured in LB solution were collected and centrifuged. The cell pellets were washed twice and resuspended in PBS (pH 7.2) at OD_{600} of 0.5, then further diluted to a final concentration of 2 $\times 10^5$ cfu/mL. Aliquots of this suspension (25 μL) were placed into a 96-well plate. PpIX and its synthesized conjugates were diluted in 25 μL PBS and then added into the bacteria suspensions to give the desired concentration. After treating with compounds at 37 °C in the dark for 2 h, the cultures were then added to 50 μL of twice-LB solution and further incubated at 37 °C for 16 h. The wells containing the same number of cells but no compounds and the wells containing the same culture solution but without bacterial cells were set as control groups. The plate was then read using a 96-well plate reader at 600 nm. The MIC value was the lowest concentration of compound that prevented the growth of bacteria.

Bacterial Cell Imaging. Bacterial strains cultured overnight in Luria−Bertani (LB) solution were harvested and washed twice with sterile phosphate-buffered saline (PBS, pH 7.2). The washed cells were resuspended in PBS with an OD_{600} of 0.7, Then 100 μL aliquots were treated with 2 μM of compounds PpIX and these two PpIX−peptide conjugates. After incubation for 20 min in the dark at 37 °C, the cells were washed with PBS by centrifugation to remove the unbound compounds and then a drop of the suspension was immobilized on poly(L-lysine)-treated coverslips followed by covering with another coverslip. Fluorescent images were acquired with confocal laser microscope (Nikon Eclipse TE2000-E, CFI VC 100× oil immersed optics), using an excitation wavelength of 488 nm and a LP filter at 650 nm.

Quantification of bacterial cell staining was performed with *Image J* software v 1.44 (NIH) according to its standard manual. Statistic analysis was carried out using *Origin* v 8.0 software. Error bars reflect the standard error of the mean.

Scheme 1. Synthesis and Characterization of PpIX−Peptide Conjugates[a]
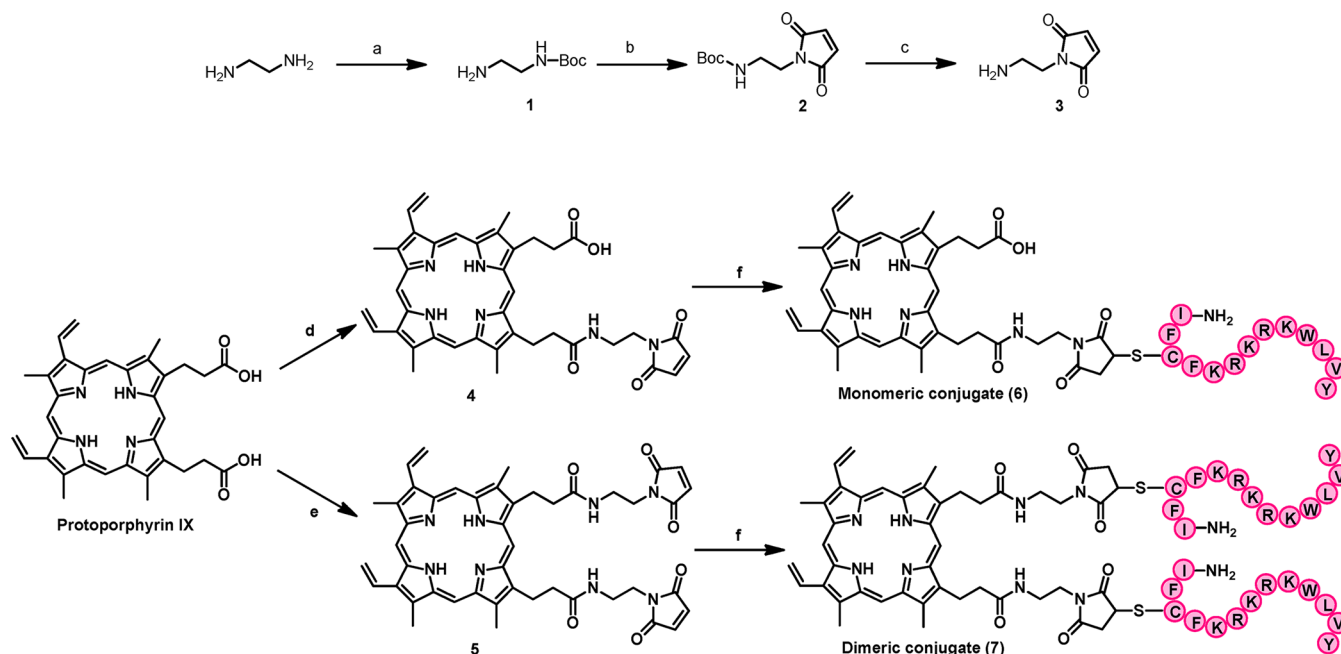
[a]Reagents and conditions: (a) Boc₂O, Et₃N, EtOH, 0 °C; (b) 1. Maleic anhydride, Et₃N, Et₂O, 0 °C; 2. Ac₂O, Na₂OAc, 60−70 °C; (c) TFA, DCM, 0 °C−rt; (d) and (e) HOSu, EDC·HCl, DMF, 0 °C−rt; (f) DIPEA, DMSO, rt.

Statistical significance (set at $P < 0.05$) was determined by Student's t test.

Selective Bacterial Cell Staining over Mammalian Cells. A mixture of live Jurkat T cells $[(0.5−1) \times 10^5$ cfu/mL] and bacteria (10^8 cfu/mL) in PBS (pH = 7.2) was incubated with 4 μM of dimeric PpIX−peptide conjugate 7 at 37 °C for 10 min. After being harvested by centrifugation (5 min at 500 g for Jurkat T cells and then 5 min at 3000 g for bacterial cells), the pellets of both mammalian and bacterial cells were mixed again in PBS, and 8 μL of the suspensions was added to a poly(L-lysine)-coated coverslip followed by slightly covering with another coverslip for immobilization. The images were taken as described above.

Photodynamic Inactivation against Bacterial Cells. Bacteria were grown and washed as imaging and MIC tests. From OD$_{600}$ of 0.7 in PBS, the bacteria suspension was diluted to a final concentration of 2×10^8 cfu/mL. 60 μL aliquots of this suspension were mixed with the compounds (in 60 μL PBS) and then added into the wells of the 96-well plate made up the calculated concentration of compound (0, 0.25, 0.5, 1.0, or 2.0 μM). The plate was incubated in the dark at 37 °C for 20 min. Before irradiation, 20 μL aliquots from each well were pipeted out and further diluted to a series of sample concentrations from 10^7 cfu/mL to 10^4 cfu/mL. The remaining was exposed to a white light source for 2, 5, and 10 min, and then again, 20 μL aliquots from each well were diluted to the same series of concentrations after the specific light exposure time. Twenty-five microliter aliquots of each suspension of bacteria were subsequently plated onto LB agar plates then incubated at 37 °C overnight. The number of colony-forming units was counted after incubation and plotted onto a log scale.

Phototoxicity of Conjugate 7 toward Jurkat T Cells. The cell toxicity assay was performed using the Tox-8 assay (Sigma Aldrich) according to the manufacturer's instructions and the reported method.[39] In brief, Jurkat T cells were cultured in 96-well plates at a density of 2×10^4 cells/well, and

then were incubated with the dimeric PpIX−peptide conjugate (7) with varying concentrations at 37 °C for 20 min. After incubation, the cells were exposed to a white light source for 10 min (30 J/cm²), and then incubated for a further 24 h in the dark. As for the dark control assays, the plate was kept in the dark during the whole process. After removing the conjugate 7 containing medium by centrifugation, the cells were incubated with the Tox-8 reagent. After two hours' incubation, the absorbance was measured at the wavelength of 600 nm by a Tecan Infinite M200 microplate reader. The measurement at the wavelength of 690 nm was set as reference, which was subtracted from the 600 nm measurement later. The wells without cells but with Tox-8 reagent were used as controls. Each experiment was performed in quintuplicate.

RESULTS AND DISCUSSION

Chemistry and Spectroscopic Studies. Scheme 1 illustrated the synthetic pathway for the preparation of porphyrin and peptide derivatives. Typically, unlike the Gram-positive organisms, the cell wall of Gram-negative strains contains LPS in the outer membrane, which generally acts as a protective permeability barrier. The LPS component increases the negative charge in the cell wall, thus reducing the binding effect of many neutral and anion drugs. In our previous work, we described a series of de novo designed antimicrobial and anti-endotoxic peptides. These peptides selectively interacted with negatively charged lipids including LPS and adopted β-boomerang structures in LPS micelles.[40] As a mode of action, these peptides destabilized LPS structures and penetrated into the outer membrane of Gram-negative bacterial strains. In this study, we chose an analogue of the β-boomerang antimicrobial peptide YI13WF with the sequence of YVLWKRKRKFCFI-Amide as target ligand due to the higher affinity to neutralize LPS in Gram-negative bacterial membrane. The designed peptide sequence was prepared based on the standard solid-
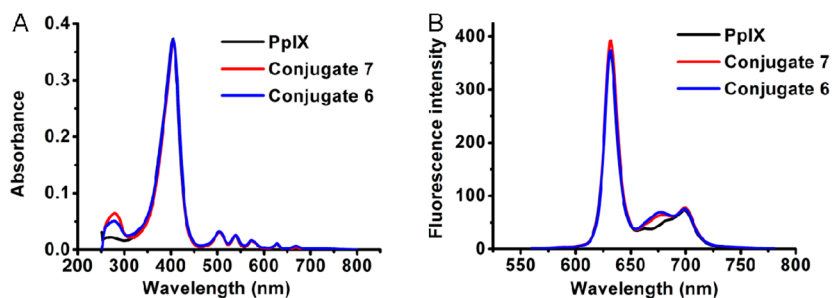
Figure 1. UV−vis absorption and fluorescent emission spectrum. (A) Absorption at concentration of 5.0 μM in DMSO; (B) emission spectrum excited at 504 nm at same concentration.

phase preparation through a commercial source. Considering a single cysteine residue in the peptide sequence, a thiol-reactive maleimide group was first introduced into the PpIX structure through ethylenediamine as the linkage to yield the maleimide-modified monomeric PpIX intermediates **4**, which could further react with the cysteine residue in the peptide sequence to afford the PpIX−peptide conjugate through the specific interaction between free thiol and maleimide group. A simple reverse-phase HPLC purification produced the monomeric PpIX-peptide derivative **6** with the yield of 56%. Similarly, the dimeric peptide adduct with PpIX moiety was also prepared in 48% yield by conjugating the bimaleimide PpIX intermediate **5** with excess YI13WF peptide sequence. The final products **6** and **7** were purified to >95% purity (Supporting Information Figure S1) by reverse-phase HPLC and further characterized by NMR and mass spectrometry (ESI-MS).

After obtaining the porphyrin−peptide derivatives, their photochemical properties were investigated by UV−vis absorption and fluorescence spectra. The spectroscopic characterization demonstrated that both the monomeric and dimeric PpIX-conjugates exhibited similar absorptions from 330 to 650 nm with an intense soret band near 400 nm and four Q-band peaks between 500 and 620 nm (Figure 1A). The emission spectra of monomeric and dimeric peptide PpIX−peptide conjugates are similar and showed no difference from those of PpIX molecule (Figure 1B). The results indicated that the peptide conjugation has no significant effect on the fluorescent properties of PpIX molecule. Moreover, the PpIX−peptide conjugates together with PpIX could also produce reactive oxygen species (e.g., singlet oxygen, etc.) when excited by white light irradiation, which were determined by the standard assay based on the specific probe of 9,10-anthracennediyl-bis(methylene) dimalonic acid (ABDA) reported previously (Supporting Information Figure S2).[19,21,22]

MIC Tests. The antibacterial studies were first carried out by investigating the minimum inhibitory concentration (MIC) of PpIX-peptide derivatives. In order to avoid the potential interferences of photoexcitation during the MIC tests, the MIC experiments were performed in the dark. In a typical study, four standard Gram-negative bacteria including *E. coli* DH5a (ATCC 53868), *S. enterica* (ATCC 14028), and ampicillin-resistant bacterial strains *E. coli* BL21 (Amp^r *E. coli*) and *K. pneumoniae* (ATCC 700603) were used as model organisms. As expected, the antimicrobial peptide sequence, YI13WF, demonstrated potent MIC activity against these Gram-negative bacterial strains mostly attributed to its stronger binding effect toward lipids exists at the outer membrane of Gram-negative bacteria.[29,40] Compared to the parent peptide sequence, monomeric PpIX-peptide derivative showed a similar trend to

inhibit bacterial growth (Table 1), suggesting that conjugation of PpIX to the peptide would not affect the binding affinity

Table 1. MIC Values of PpIX, Free Peptide YI13WF, and PpIX-YI13WF Conjugates

	MIC (μM)			
	E. coli DH5a	*E. coli* BL-21	*K. pneumoniae*	*S. enterica*
Conjugate 7	2	4	8	4
Conjugate 6	8	32	32	32
YI13WF	8	32	32	~ 24
PpIX	>64	>64	>64	>64

between the antimicrobial peptide and LPS moieties on the bacterial membranes. Under the same assay conditions, the MIC value of dimeric PpIX-peptide against bacterial strains was found to be 4- to 8-fold less than that of YI13WF peptide or monomeric PpIX-YI13WF derivative, indicating that the greater potency of bacterial inactivation could be caused by the dimeric derivative. As control, similar antimicrobial activity was also evaluated by using the PpIX molecule alone (Table 1). The higher MIC value of PpIX clearly demonstrated the limited activity to inhibit the bacterial growth, which was consistent with the bacterial inactivation results reported previously.[17−26]

Bacterial Imaging Studies. In order to verify the binding affinity of PpIX-peptide derivatives toward various Gram-negative bacterial strains, living cell imaging was conducted under a confocal microscope upon laser excitation of the Q-band absorbance of PpIX. In this study, the bacterial strains were incubated with PpIX−peptide conjugates as described in the experiment section. As show in Figure 2A, the bacterial strains incubated with PpIX itself did not show any obvious fluorescence. However, after incubation of the bacterial strains with PpIX−peptide conjugates, the confocal microscope indicated a significant fluorescent imaging of the bacterial cells stained with both dimeric and monomeric PpIX−peptide conjugates. In contrast to the monomeric conjugate **6** and free PpIX, the dimeric conjugate **7** exhibited stronger fluorescence, suggesting a higher binding ability of dimeric peptide conjugate toward the surface of bacterial strains. The different staining effects of the tested compounds were further quantified by measuring the fluorescence imaging intensity.[41] As shown in Figure 2B, fluorescence intensity from the monomeric PpIX-peptide stained cells is about 8 times greater than that of free PpIX stained cells, and such a difference would even increase up to about 20 times when the same bacterial strains were stained with dimeric PpIX−peptide conjugate, suggesting an even higher binding association between the dimeric peptide conjugate and Gram-negative bacteria. By contrast, the
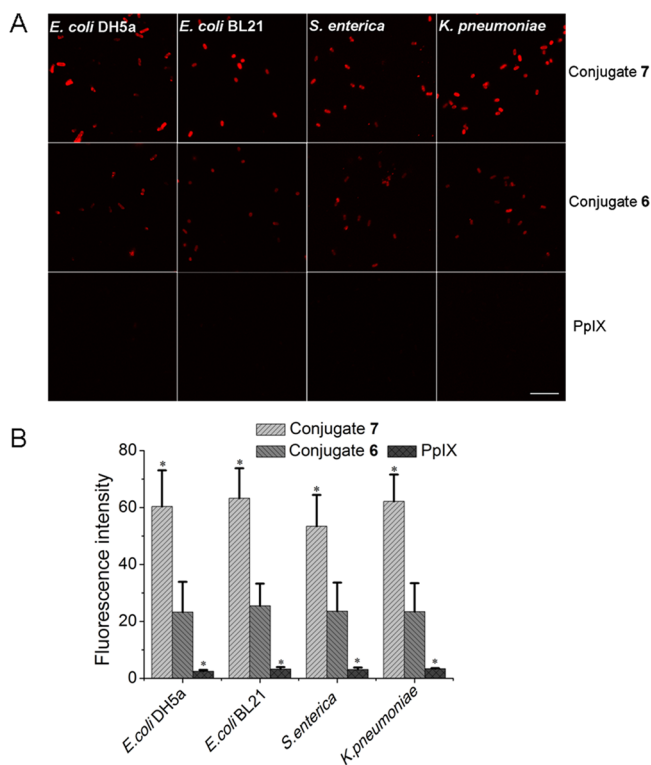
Figure 2. Fluorescent imaging of bacterial staining with PpIX and its derivatives. (A) The bacterial cells were treated with 2 μM compounds at room temperature for 10 min. Excitation wavelength was 488 nm, and fluorescence was detected using a long-pass filter at 650 nm. Scale bar = 10 μm. (B) Quantitative analysis of bacterial staining, mean $\pm$ S.E. * $P < 0.05$ versus the monomeric conjugate.

incubation of porphyrin itself with bacterial strains would not result in obvious fluorescence signals, mostly due to the weak binding affinity of porphyrin molecules with LPS moieties on the surface of Gram-negative bacteria. The living bacterial imaging and fluorescent intensity measurements clearly confirmed the hypothesis that antimicrobial peptide sequence YI13WF may act as affinity ligands for specific targeting the surface of Gram-negative bacterial strains. The enhanced bacterial imaging and bacterial MIC inactivation properties observed in the living cells treated with dimeric porphyrin−peptide conjugate may be attributable to the multivalent effects.[18,42−46]

Encouraged by the effective bacterial imaging results, the dimeric PpIX−peptide conjugate was further applied to investigate the possibility of selective recognition and imaging of bacterial strains over mammalian cells. As proof-of-concept, the Jurkat T cells were chosen and co-cultured with different Gram-negative bacteria such as Amp[r] E. coli and K. pneumonia, respectively, and then incubated with dimeric PpIX−peptide conjugate at 37 °C for 10 min. The bacterial and cellular imaging measurements were acquired by using a confocal fluorescence microscope. As shown in Figure 3, for both mixtures of Jurkat T cells with Amp[r] E. coli and Jurkat T cells with K. pneumonia, the significant red fluorescence could only be observed in bacteria, and there was no obvious fluorescence detected in Jurkat T cells (Figure 3 and Supporting Information Figure S4). The higher fluorescence observed in bacteria clearly indicated the ability of the dimeric PpIX−peptide conjugate to selectively recognize and image bacterial strains over mammalian cells. Generally, phosphatidylcholine (PC) and phospha-
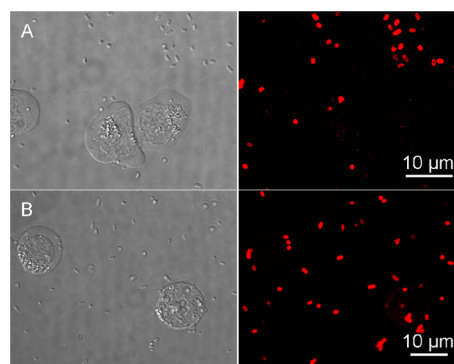

Figure 3. Fluorescent images of Jurkat T cells and two antibiotic-resistant Gram-negative bacteria: (A) E. coli BL21 and (B) K. pneumoniae incubated with conjugate 7 (4 μM). Left: bright field images, right: fluorescent images. The fluorescence of PpIX is highlighted in red.

tidylserine (PS) are commonly found lipid components located at the exoplasmic leaflet and inner leaflet of the plasma membrane of mammalian cells, respectively. Compared to the different phospholipids in the mammalian cell membranes, the major components of LPS located at the surface of Gram-negative bacterial strains would be the main reason to greatly contribute the selective recognition of dimeric PpIX−peptide conjugate to bacterial strains instead of mammalian cells.[37]

Photodynamic Bacterial Inactivation Studies. To demonstrate that the PpIX-peptide derivatives are effective for the photodynamic inactivation of bacterial growth, the PACT treatment was conducted by exposure of Gram-negative strains with white light illumination in the presence of PpIX−peptide conjugates. Upon white light irradiation, the bacteria lethality was evaluated by counting the number of colony forming units (cfu) on the LB agar plate. It is found that both of the monomeric and dimeric PpIX−peptide conjugates displayed effective photoinactivation to the tested bacterial strains including those strains (e.g., ampicillin-resistant E. coli BL2l and K. pneumoniae) with drug resistance properties. In contrast to the monomeric PpIX−peptide conjugate, the dimeric one showed that higher antibacterial activity and more than 99% bacterial lethality (>2.0 $\log_{10}$ reduction) could be observed at only 0.5 μM after 30 J/cm^2 of light irradiation (Figure 4A,C), whereas the control studies without light irradiation only showed limited bacterial lethality. Under a fixed concentration (0.5 μM) of photosensitizers, these two PpIX−peptide conjugates also demonstrated even more significant bacterial reduction when higher doses of light irradiation were employed (Figure 4A,B). This photodynamic bacterial inactivation indicated more potent activity than the MIC values of dimeric PpIX−peptide conjugate observed for E. coli DH5a (∼4 times) and S. enterica (∼8 times) including other Gram-negative strains such as ampicillin-resistant E. coli BL21 (∼8 times) and K. pneumoniae (∼16 times). Moreover, the efficacy of bacterial photoinactivation was also found to be concentration-dependent, where the significant bacterial killing with more than 99.9% bacterial lethality (>3.0 $\log_{10}$ reduction) could still be easily obtained when photodynamic inactivation was conducted in the presence of higher concentrations of dimeric PpIX−peptide conjugate (Figure 4 and Supporting Information Figure S3). In contrast, the presence of free PpIX alone would not produce any detectable bacterial inactivation when the bacterial strains were treated with identical white light
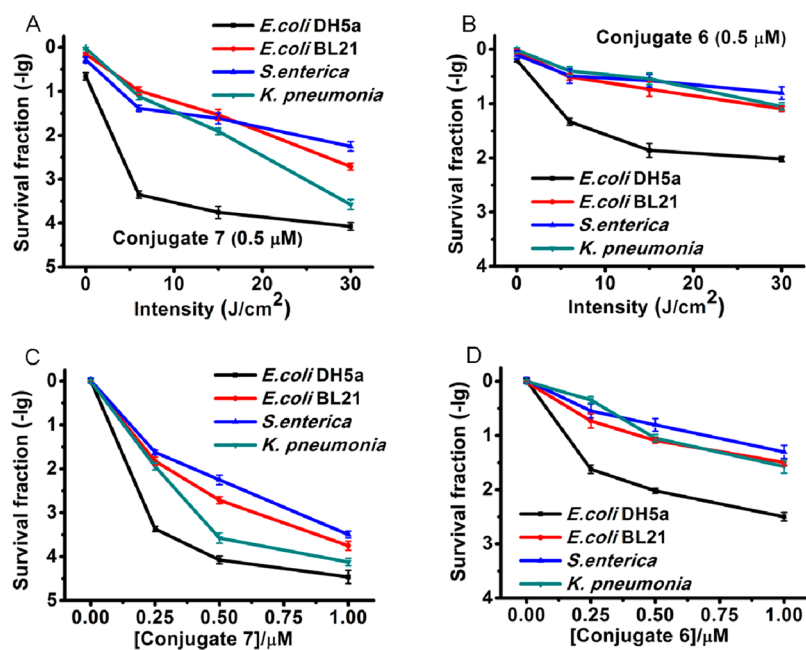
Figure 4. Bacterial photoinactivation with PpIX−peptide conjugates. (A and B) Dose effects in light-induced toxicity against bacterial cells at the fixed concentarion (0.5 µM) of PpIX−peptide conjugates **7** and **6**. (C and D) Survival curves of the bacterial cells treated with several concentrations of PpIX−peptide conjugates **7** and **6** at the fixed energy of irradiation (30 J/cm^2). *E. coli* DH5a (■), *E. coli* BL21 (●), *S. enterica* (▲), and *K. pneumoniae* (▼).

irradiation (Supporting Information Figure S3). A similar mammalian cell viability analysis toward Jurkat T cells with and without white light irradiation was also conducted by using Tox-8 assay. There were no significant mammalian cell viabilities changed with the increase of dimeric PpIX-peptide concentration and no obvious cytotoxicity detected for both the light irradiation and dark conditions (Supporting Information Figure S5). These results clearly supported our hypothesis that PpIX-conjugated dimeric peptide derivative could serve as an effective reagent to inactivate Gram-negative bacteria over mammalian cells, mostly owing to the higher binding affinity of the dimeric peptide sequence toward the LPS moieties on the surface of bacterial strains, which may lead to the locally high concentration of photosensitizers caused by the efficient polyvalent/multivalent interactions. The high concentration of dimeric porphyrin peptide conjugate accumulated at close proximity to the bacterial surface could thus constitute significant bacterial lethality upon exposure to some dose of light illumination.

CONCLUSIONS

In this work, we have successfully constructed a simple and specific strategy for effective fluorescent imaging and photo-dynamic inactivation of Gram-negative bacterial strains through the conjugation of photosensitizer protoporphyrin IX (PpIX) with two lipopolysaccharide (LPS) neutralizing peptide sequences: YI13WF (YVLWKRKRKFCFI-Amide). By taking advantage of the higher binding affinity of the peptide sequence toward the LPS components, the dimeric PpIX peptide conjugate can effectively deliver the photosensitizer to the surface of Gram-negative bacterial strains and thus enhance the local concentration through the effects of multivalency. Upon the white light illumination, the dimeric PpIX−peptide derivative indicated the potent activity against Gram-negative bacterial pathogens including those with drug-resistant proper-

ties, which is more active than the MIC values of YI13WF peptide and PpIX alone. Apart from the higher photodynamic antimicrobial application, the dimeric PpIX−peptide conjugate also displayed the promising function in real-time fluorescent imaging of living bacterial strains. Moreover, both fluorescent imaging and photoinactivation experiments also demonstrated that the dimeric PpIX-YI13WF conjugate could selectively target bacterial strains over mammalian cells and generate less damage to mammalian cells. The demonstrated strategy based on the dimeric lipids affinity peptide sequence derivative may provide the great possibility for further study of biological functions in Gram-negative bacterial strains under living settings. It may also supply the potential alternative for the effective inactivation of bacterial pathogens especially for those with drug-resistant properties.

ASSOCIATED CONTENT

Ⓢ Supporting Information

HPLC analysis of peptide conjugates, measurement of singlet oxygen generation, controlled bacterial and cellular photo-inactivation, controlled bacterial and cellular fluorescent imaging, bacterial imaging and fluorescent intensity quantifica-tion, ^{1}H NMR for compounds **1**, **2**, **4−7**, and ESI-MS for compounds **6** and **7**. This material is available free of charge via the Internet at http://pubs.acs.org.

AUTHOR INFORMATION

Corresponding Author

*Xing Bengang: Phone 65-63168758, e-mail bengang@ntu.edu. sg. S. Bhattacharjya: Phone 65-63167997, e-mail surajit@ntu. edu.sg.

Notes

The authors declare no competing financial interest.

■ ABBREVIATIONS:

PACT, photodynamic antimicrobial chemotherapy; HPLC, high-performance liquid chromatography; LPS, lipopolysaccharide; PpIX, protoporphyrin IX; MIC, minimum inhibitory concentration.

■ REFERENCES

(1) Walsh, C. T. (2003) *Antibiotics: actions, origins, and resistance*, pp 195−220, ASM Press, Washington, DC.

(2) Spencer, J., and Walsh, T. R. (2006) A new approach to the inhibition of metallo-beta-lactamases. *Angew. Chem., Int. Ed. 45*, 1022−1026.

(3) Fisher, J. F., Meroueh, S. O., and Mobashery, S. (2005) Bacterial resistance to beta-lactam antibiotics: compelling opportunism, compelling opportunity. *Chem. Rev. 105*, 395−424.

(4) Xing, B. G., Rao, J. H., and Liu, R. (2008) Novel beta-lactam antibiotic derivatives: their new applications as gene reporters, antitumor prodrugs, and enzyme inhibitors. *Mini-Rev. Med. Chem. 8*, 455−471.

(5) Maiti, S. N., Phillips, O. A., Micetich, R. G., and Livermore, D. M. (1998) Beta-lactamase inhibitors: agents to overcome bacterial resistance. *Curr. Med. Chem. 5*, 441−456.

(6) Jiang, T., Liu, R., Huang, X., Feng, H., Teo, W., and Xing, B. G. (2009) Colorimetric screening of bacterial enzyme activity and inhibition based on the aggregation of gold nanoparticles. *Chem. Commun. 15*, 1972−1974.

(7) Dolmans, D. E., Fukumura, D., and Jain, R. K. (2003) Photodynamic therapy for cancer. *Nat. Rev. Cancer 3*, 380−387.

(8) Detty, M. R., Gibson, S. L., and Wagner, S. J. (2004) Current clinical and preclinical photosensitizers for use in photodynamic therapy. *J. Med. Chem. 47*, 3897−3915.

(9) Castano, A. P., Mroz, P., and Hamblin, M. R. (2006) Photodynamic therapy and anti-tumour immunity. *Nat. Rev. Cancer 6*, 535−545.

(10) Wu, S., Chang, E., and Cheng, Z. (2011) Molecular probes for bioluminescence imaging. *Curr. Org. Synth. 8*, 488−497.

(11) Lovell, J. F., Liu, T. W., Chen, J., and Zheng, G. (2010) Activatable photosensitizers for imaging and therapy. *Chem. Rev. 110*, 2839−2857.

(12) Ragas, X., Copper, L. P., White, J. H., Nonell, S., and Flors, C. (2011) Quantification of photosensitized singlet oxygen production by a fluorescent protein. *ChemPhysChem 12*, 161−165.

(13) Shao, Q., and Xing, B. G. (2010) Photoactive molecules for applications in molecular imaging and cell biology. *Chem. Soc. Rev. 39*, 2835−2846.

(14) Philips, D. (2011) Toward targeted photodynamic therapy. *Pure Appl. Chem. 83*, 733−748.

(15) Celli, J. P., Spring, B. Q., Rizvi, I., Evans, C. L., Samkoe, K. S., Verma, S., Pogue, B. W., and Hasan, T. (2010) Imaging and photodynamic therapy: mechanisms, monitoring, and optimization. *Chem. Rev. 110*, 2795−2838.

(16) Wainwright, M. (1998) Photodynamic antimicrobial chemotherapy (PACT). *J. Antimicrob. Chemother. 42*, 13−28.

(17) Suci, P. A., Varpness, Z., Gillitzer, E., Douglas, T., and Young, M. (2007) Targeting and photodynamic killing of a microbial pathogen using protein cage architectures functionalized with a photosensitizer. *Langmuir 23*, 12280−12286.

(18) Strassert, C. A., Otter, M., Albuquerque, R. Q., Hone, A., Vida, Y., Maier, B., and De Cola, L. (2009) Photoactive hybrid nanomaterial for targeting, labeling, and killing antibiotic-resistant bacteria. *Angew. Chem., Int. Ed. 48*, 7928−7931.

(19) Xing, C. F., Xu, Q. L., Tang, H. W., Liu, L. B., and Wang, S. (2009) Conjugated polymer/porphyrin complexes for efficient energy transfer and improving light-activated antibacterial activity. *J. Am. Chem. Soc. 131*, 13117−13124.

(20) Gad, F., Zahra, T., Francis, K. P., Hasan, T., and Hamblin, M. R. (2004) Targeted photodynamic therapy of established soft-tissue infections in mice. *Photochem. Photobiol. Sci. 3*, 451−458.

(21) Xing, B. G., Jiang, T., Bi, W., Yang, Y., Li, L., Ma, M., Chang, C. K., Xu, B., and Yeow, E. K. L. (2011) Multifunctional divalent vancomycin: the fluorescent imaging and photodynamic antimicrobial properties for drug resistant bacteria. *Chem. Commun. 47*, 1601−1603.

(22) Shao, Q., and Xing, B. G. (2012) Enzyme responsive luminescent ruthenium (II) cephalosporin probe for intracellular imaging and photoinactivation of antibiotics resistant bacteria. *Chem. Commun. 48*, 1739−1741.

(23) Hope, C. K., Packer, S., Wilson, M., and Nair, S. P. (2009) The inability of a bacteriophage to infect Staphylococcus aureus does not prevent it from specifically delivering a photosensitizer to the bacterium enabling its lethal photosensitization. *J. Antimicrob. Chemother. 64*, 59−61.

(24) Perni, S., Prokopovich, P., Pratten, J., Parkin, I. P., and Wilson, M. (2011) Nanoparticles: their potential use in antibacterial photodynamic therapy. *Photochem. Photobiol. Sci. 10*, 712−720.

(25) Zhu, C., Yang, Q., Liu, L., Lv, F., Li, S., Yang, G., and Wang, S. (2011) Multifunctional cationic poly(p-phenylene vinylene) polyelectrolytes for selective recognition, imaging, and killing of bacteria over mamalian cells. *Adv. Mater. 23*, 4805−4810.

(26) Bonnett, R., Buckley, D. G., Burrow, T., Galia, A. B. B., Saville, B., and Songca, S. P. (1993) Photobactericidal materials based on porphyrins and phthalocyanines. *J. Mater. Chem. 3*, 323−324.

(27) Raetz, C. R., and Whitfield, C. (2002) Lipopolysaccharide endotoxins. *Annu. Rev. Biochem. 71*, 365−700.

(28) Hancock, R. E. (1997) The bacterial outer membrane as a drug barrier. *Trends. Microbiol. 5*, 37−42.

(29) Bhattacharjya, S. (2010) *De novo* designed lipopolysaccharide binding peptides: structure based development of antiendotoxic and antimicrobial drugs. *Curr. Med. Chem. 17*, 3080−3093.

(30) Beutler, B., and Rietschel, E. T. (2003) Innate immune sensing and its roots: the story of endotoxin. *Nat. Rev. Immunol. 3*, 169−176.

(31) Cohen, J. (2002) The immunopathogenesis of sepsis. *Nature 420*, 885−891.

(32) Hardaway, R. M. (2000) A review of septic shock. *Am. Surg. 66*, 22−29.

(33) Hancock, R. E., and Scott, M. G. (2000) The role of antimicrobial peptides in animal defenses. *Proc. Natl. Acad. Sci. U.S.A. 97*, 8856−8861.

(34) Dürr, U. H., Sudheendra, U. S., and Ramamoorthy, A. (2006) LL-37, the only human member of the cathelicidin family of antimicrobial peptides. *Biochem. Biophys. Acta 1758*, 1408−1425.

(35) Rosenfeld, Y., Papo, N., and Shai, Y. (2006) Endotoxin (lipopolysaccharide) neutralization by innate immunity host-defense peptides. *J. Biol. Chem. 281*, 1636−1643.

(36) Bourre, L., Giuntini, F., Eggleston, I. M., Mosse, C. A., Macrobert, A. J., and Wilson, M. (2010) Effective photoinactivation of Gram-positive and Gram-negative bacterial strains using an HIV-1 Tat peptide-porphyrin conjugate. *Photochem. Photobiol. Sci. 9*, 1613−1620.

(37) Zasloff, M. (2002) Antimicrobial peptides of multicellular organisms. *Nature 415*, 389−395.

(38) Zou, G., De Leeuw, E., Li, C., Pazgier, M., Li, C., Zeng, P., Lu, W.-Y., Lubkowski, J., and Lu, W. (2007) Toward understanding the cationicity of defensins. *J. Biol. Chem. 282*, 19653−19665.

(39) Liu, D. (1981) A rapid biochemical test for measuring chemical toxicity. *Bull. Environ. Contam. Toxicol. 26*, 145−149.

(40) Bhunia, A., Mohanram, H., Domadia, P. N., Torres, J., and Bhattacharjya, S. (2009) Designed β-boomerang antiendotoxic and antimicrobial peptides. *J. Biol. Chem. 284*, 21991−22004.

(41) Hamilton, N. (2009) Quantification and its application in fluorescent microscopy imaging. *Traffic 10*, 951−961.

(42) Perni, S., Prokopovich, P., Pratten, J., Parkin, I. P., and Wilson, M. (2011) Nanoparticles: their potential use in antibacterial photodynamic therapy. *Photochem. Photobiol. Sci. 10*, 712−720.

(43) Bombelli, C., Bordi, F., Ferro, S., Giansanti, L., Jori, G., Mancini, G., Mazzuca, C., Monti, D., Ricchelli, F., Sennato, S., and Venanzi, M. (2008) New cationic liposomes as vehicles of m-tetrahydroxyphenyl-chlorin in photodynamic therapy of infectious diseases. *Mol. Pharmaceutics 5*, 672−679.

(44) Li, L. H., and Xu, B. (2005) Multivalent vancomycins and related antibiotics against infectious diseases. *Curr. Pharm. Des. 11*, 3111−3124.

(45) Liu, S. P., Zhou, L., Lakshminarayanan, R., and Beuerman, R. W. (2010) Multivalent antimicrobial peptides as therapeutics: design principles and structural diversities. *Int. J. Pept. Res. Ther. 16*, 199−213.

(46) Pieters, R. J., Arnusch, C. J., and Breukink, E. (2009) Membrane permeabilization by multivalent anti-microbial peptides. *Protein Pept. Lett. 16*, 736−742.